

A new heuristics model of simulating pedestrian dynamics based on Voronoi diagram

Xin-Sen Wu(武鑫森), Hao Yue(岳昊), Qiu-Mei Liu(刘秋梅), Xu Zhang(张旭), and Chun-Fu Shao(邵春福)
Citation: Chin. Phys. B, 2021, 30 (**1**): 018902. DOI: 10.1088/1674-1056/abb3f5
Journal homepage: http://cpb.iphy.ac.cn; http://iopscience.iop.org/cpb

What follows is a list of articles you may be interested in

An extended cellular automata model with modified floor field for evacuation

Da-Hui Qin(秦大辉), Yun-Fei Duan(段云飞), Dong Cheng(程栋), Ming-Zhu Su(苏铭著), Yong-Bo Shao(邵永波)
Chin. Phys. B, 2020, 29 (**9**): 098901. DOI: 10.1088/1674-1056/abad1b

Influence of bottleneck on single-file pedestrian flow: Findings from two experiments

Cheng-Jie Jin(金诚杰), Rui Jiang(姜锐), Da-Wei Li(李大韦)
Chin. Phys. B, 2020, 29 (**8**): 088902. DOI: 10.1088/1674-1056/ab8da3

Pedestrian choice behavior analysis and simulation of vertical walking facilities in transfer station

Yong-Xing Li(李永行), Hong-Fei Jia(贾洪飞), Jun Li(李军), Ya-Nan Zhou(周亚楠), Zhi-Lu Yuan(原志路), Yan-Zhong Li(李延忠)
Chin. Phys. B, 2016, 25 (**10**): 108901. DOI: 10.1088/1674-1056/25/10/108901

Dynamic feature analysis in bidirectional pedestrian flows

Xiao-Xia Yang(杨晓霞), Winnie Daamen, Serge Paul Hoogendoorn, Hai-Rong Dong(董海荣), Xiu-Ming Yao(姚秀明)
Chin. Phys. B, 2016, 25 (**2**): 028901. DOI: 10.1088/1674-1056/25/2/028901

A new collision avoidance model for pedestrian dynamics

Wang Qian-Ling, Chen Yao, Dong Hai-Rong, Zhou Min, Ning Bin
Chin. Phys. B, 2015, 24 (**3**): 038901. DOI: 10.1088/1674-1056/24/3/038901

A new heuristics model of simulating pedestrian dynamics based on Voronoi diagram*

Xin-Sen Wu(武鑫森)[1], Hao Yue(岳昊)[1,†], Qiu-Mei Liu(刘秋梅)[1], Xu Zhang(张旭)[2], and Chun-Fu Shao(邵春福)[1]

[1] *Key Laboratory of Transport Industry of Big Data Application Technologies for Comprehensive Transport, Ministry of Transport, Beijing Jiaotong University, Beijing* 100044, *China*

[2] *College of Civil Engineering and Architecture, Henan University of Technology, Zhengzhou* 450001, *China*

(Received 12 July 2020; revised manuscript received 24 August 2020; accepted manuscript online 1 September 2020)

A new heuristics model based on the Voronoi diagram is presented to simulate pedestrian dynamics with the non-crowded state, in which these mechanisms of preference demand evading and surpassing, microscopic anti-deadlock, and site-fine-tuning are considered. The preference demand describes the willingness determination of detouring or following other pedestrians. In the evading and surpassing mechanisms, in order to achieve a balance between avoiding conflicts and minimizing detour distances, a new pair of concepts: "allow-areas and denial-areas" are introduced to divide the feasible region for pedestrians detour behaviors, in which the direction and magnitude of detour velocity are determined. A microscopic anti-deadlock mechanism is inserted to avoid deadlock problem of the counter-directional pedestrian. A site-fine-tuning mechanism is introduced to describe the behavior of avoiding getting too close to the neighbors in pedestrian movement. The presented model is verified through multiple scenarios, including the uni- or bi-direction pedestrian flow in the corridor without obstacles, the uni-direction pedestrian flow in the corridor with obstacles, and the pedestrian evacuation from a room with single-exit. The simulation results show that the velocity–density relationship is consistent with empirical data. Some self-organizing phenomena, such as lanes formation and arching are observed in the simulation. When pedestrians detour an obstacle, the avoiding area before the obstacle and the unoccupied area after the obstacle can be observed. When pedestrians evacuate through a bottleneck without panic, the fan-shaped crowd can be found, which is consistent with the actual observation. It is also found that the behavior of following others in an orderly manner is more conducive to the improvement of the overall movement efficiency when the crowd moves in a limited space.

Keywords: pedestrian dynamics, pedestrian simulation, heuristics rules, Voronoi diagram

PACS: 89.40.–a, 05.65.+b, 07.05.Tp **DOI:** 10.1088/1674-1056/abb3f5

1. Introduction

With the continuous development of urbanization, the gathering and transfer activities of pedestrians in walking facilities are becoming more and more frequent. Generally, the improper design of walking facilities and the unreasonable organization of pedestrian flow can reduce the efficiency of pedestrian movement and even induce the stampede-rush phenomena of pedestrians in panic situations. Therefore, the issue of pedestrian evacuation in large public facilities is getting more and more attention, and the research interest in pedestrian dynamics is increasing. Furthermore, these studies of the characteristics of pedestrian movement, the design of walking facilities,[1,2] the organization of pedestrian flow, and the strategies of pedestrian evacuation[3–5] are of great significance. Meanwhile, with the development of computer technology, researchers can qualitatively and quantitatively analyze the characteristics of pedestrian flow[6] and reproduce the macroscopic phenomena of crowds in pedestrian simulation. Then the technology of pedestrian simulation has become a primary method to explore the microscopic and macroscopic characteristics of pedestrian flow.[7]

According to the characteristics of the space division, pedestrian simulation models mainly include discrete-space and continuous-space models. Meanwhile, according to the driving methods, the simulation methods mainly include force-based and rule-based models.[8] They are widely used to research the microscopic and macroscopic characteristics of pedestrians. Among them, the discrete-space models have the characteristics of discretization in the simulation space and step, such as the cellular automata (CA) model,[9–13] the floor field model,[14,15] the lattice gas model,[16] and the dynamic parameters model.[17–19] The continuous-space models have the characteristics of discrete simulation step and continuous simulation space, such as the social force model (SFM),[20–33] the centrifugal force model.[34] The SFM is mainly based on the force and the heuristic model is mainly based on the rule.[8] Generally speaking, research objects mainly include pedestrians movement or evacuation in walking facilities (such as walking corridors or evacuation rooms) where we could observe the unidirectional or bidirectional pedestrian flow,[25,26]

*Project supported by the National Natural Science Foundation of China (Grant Nos. 71771013 and 71621001), in part by the National Key Research and Development Program of China (Grant No. 2019YFF0301403), in part by the Singapore Ministry of Education (MOE) AcRF Tier 2 (Grant No. MOE2016-T2-1-044), and in part by the Fundamental Research Funds for the Central Universities, China (Grant NO. 2019JBM041).

†Corresponding author. E-mail: hyue@bjtu.edu.cn

© 2021 Chinese Physical Society and IOP Publishing Ltd

the evacuation flow[23,24] with sight affected,[20] with multiple emergency exits,[35] and with spatial obstacles.[31,32] Besides, we could observe many pedestrian self-organization phenomena in the pedestrian simulation, such as "automatic canalization,"[20,21] "lane formation,"[20,21] "arching before a bottleneck,"[20,21] "fast is slow,"[10,11] and "avoiding triangle areas."[36]

Among the existing simulation models, the CA model is a discrete-space model, which is widely used because it has simple rules, fast running speed, and owns the ability to reproduce many macroscopic phenomena. It divides the space into a series of uniform discrete cells. Usually, each pedestrian occupies a cell. And update rules are set to prompt pedestrians to move to adjacent cells according to the transition probability of each time step. With the development of the CA model, Burstedde *et al.*[14] proposed the floor field model based on static and dynamic fields to simulate collective movement behaviors and self-organization phenomena of unidirectional and bidirectional pedestrian flow in many scenarios. Yue and Wang *et al.*[18] proposed the dynamic parameter model by introducing affected vision fields and describing blind follow behaviors of pedestrians during evacuation.

In contrast, the SFM is a continuous-space model which has simple rules and easy extensibility. And, it can reproduce many typical self-organizing phenomena, such as "arching before exit," "fast is slow," "gathering behavior," and other macroscopic phenomena.[20,21] The simulation result of SFM is very consistent with empirical research. The SFM proposes a concept of the imaginary social force to represent the interaction relationship between pedestrians. According to Newtonian mechanics, the performance of pedestrian movement is quantitatively affected by the combined force of self-driving force, repulsive force, and contact force.[20] Besides, researchers proposed many modifications to improve the performance of SFM, including the improvement of self-driving force,[23,24] the improvement of repulsive force,[25,26] the introduction of other parameters, the parameter calibration,[25–27] and so on. Yang and Dong *et al.*[23] introduced many parameters, such as the tension coefficient, the vision range, and the surrounding environment parameter. Moreover, they modified the expected direction and set the expected velocity rule of pedestrians to get a better simulation result of the characteristics of pedestrian flow. Seer *et al.*[25,26] used the actual pedestrian movement data to calibrate the repulsive force parameter and reproduce the pedestrian trajectory.

Besides, the heuristic-based methods,[8,37–41] which integrated heuristics into pedestrian modeling to handle complex situations and predict smoother pedestrian trajectories. Especially, the local density can be used to reflect the comfort level of pedestrians and trigger the pedestrian movement as an essential parameter.[8] In addition, some researchers studied the vision-based heuristic rule,[37] the spatiotemporal separation behavior,[39,40] and the velocity obstacle rule in motion planning.[41]

By comprehensive comparison of these models, the CA model has regular grid cells but pedestrians cannot move with the change of the location. Since pedestrians only can move to adjacent cells and the determination of the velocity direction and magnitude are partly limited, the CA model cannot effectively reproduce the microscopic behaviors of pedestrians. By contrast the SFM can overcome these defects of the CA model and reproduce smoother pedestrian movement trajectories. Moreover, the SFM can describe the pedestrian dynamics and the interaction relationship between pedestrians much better. Although the SFM has the definite advantages in reproducing microscopic behaviors and macroscopic phenomena of pedestrians flo, it still has some problems such as the image of the interactional force between pedestrians, the lack of accurate methods to measure the interaction relationship between pedestrians,[8] the unreasonably assign of the values of some parameters, and the overlarge value of the contact force between pedestrians than common sense. Especially, when pedestrians face several neighbors at the same time, all of the social force from every pedestrian needs to be combined, but lacks a unified method. The existing combination methods include linear, nonlinear, *etc*. The self-driving force of pedestrians is simply set to point directly to the direction of the destination.[20] The inadequate description of pedestrians' mechanism to avoid spatial obstacles or other pedestrians could prevent pedestrians from actively detouring other pedestrians. These defects usually induces many unreasonable phenomena, such as the oscillation and deadlock between pedestrians. The overlapping phenomena between pedestrians always occur in the traditional SFM, due to the limitation of kinetic force-based simulation framework, even if the simulation time step is set very small.[42]

Aiming at the issue that pedestrians cannot detour obstacles or neighbors effectively, Jia and Yue *et al.*[36] proposed the conjugated SFM which used the forward force and the lanechange force as a pair of conjugated force to replace the self-driving force. Moreover, they did not change the velocity magnitude but changed the velocity direction so that pedestrians can detour other pedestrians or obstacles. However, the model only suitable for the situation of every pedestrian faced one major obstacle so the simulation effect was not good when the pedestrian faced multiple obstacles. To solve the unreasonable phenomenon of the pedestrian overlapping, some scholars improved the traditional SFM. Seyfried,[43] Parisi[30] introduced a pedestrian stopping mechanism into the SFM. When the pedestrian deceleration situation occurred, the magnitude of the actual velocity or expected velocity must instantly be-

come zero. The mechanism reduced the overlapping phenomenon between pedestrians. Lakoba[22] developed an algorithm based on the explicit numerical integration scheme, which can prevent most people from forming the overlapping phenomenon in physical space. Li[44] analyzed the demand space of pedestrians and introduced a deceleration avoidance mechanism into the SFM, which avoided pedestrians' overlapping phenomenon to some extent, but did not achieve the actual detour behaviors of pedestrians.

Aiming at the characteristics of heuristics, we can see that heuristics are valuable in investigating and simulating pedestrian dynamics.[37,38] The intelligent method in heuristics was used to evaluate pedestrians' velocity direction and magnitude,[37] which replaced the rough calculation of imaginary non-contact force between pedestrians. It achieved much better simulation results and reproduced many classic self-organizing phenomena (such as "lane formation," "stop-and-go wave"). In the traditional heuristic method,[37] two heuristic rules of pedestrians' demand to walk quickly and safely determined the velocity direction and magnitude of pedestrians. Furthermore, Xiao[8] proposed a heuristic rule based on the Voronoi diagram for pedestrians to walk comfortably, which was assessed by the local density of pedestrians. However, the above heuristic rules do not consider the preference and willingness demand of pedestrians to detour. Meanwhile, Xiao[8] combined heuristic rules with the Voronoi diagram and proposed pedestrians' detour direction that pointed to the Voronoi node which was precisely located on the vertical line of two adjacent pedestrians. Then, pedestrians can avoid locating too close to touch with any neighbors and get the safety distance which reached the maximum distance at each Voronoi node. However, pedestrians expect to reach the destination in the shortest possible time. Then, when facing obstacles or other slow-speed neighbors, pedestrians need to find a balance between collision avoidance and minimizing detour distances. Obviously, the detour angle and distance are too large when pedestrians' detour direction directly points to the Voronoi node. Qu[45] proposed an improved SFM which based on the Voronoi diagram. He considered the location and velocity of pedestrians' neighbors and established a logit model to describe pedestrians' detour direction choice. Furthermore, the simulation result of unidirectional and bidirectional pedestrian flow showed that the model could reduce pedestrians' collision and deadlock frequency, increase pedestrians' average velocity magnitude, and predict pedestrians' detour behaviors. However, the model still has some defects, such as the occurrence of pedestrian overlapping phenomena, the desired detour direction of pedestrians only can be chosen between different Voronoi nodes, and the detour angle and distance of pedestrians are relatively large.

In summary, the CA model's shortcomings mainly include the fixed space, the presupposed rules, and the unintelligent pedestrian movement. The SFM's shortcomings mainly include the simple use of the force effect, no careful consideration of the force boundary, no detailed attention of the microscopic behavior, the unreasonable assign of the rough parameter, the lack of the active detour mechanism, no effective consideration of the multiple obstacles when detouring, the occurrence of the overlapping phenomenon, and the unrealistic occurrence of some macroscopic phenomena. Some heuristic models' defects with the Voronoi diagram mainly include the lack of effective balance of collision avoidance and minimizing detour distances and no consideration of pedestrians' preference and willingness demand.

In order to overcome these shortcomings, we propose a new heuristic model based on the geometric feature of the Voronoi diagram in this paper. We propose the mechanisms of preference demand, evading and surpassing, microscopic anti-deadlock, and site-fine-tuning. The characteristics of our model mainly include the dynamic space segmentation, the change of every space shape with the pedestrian movement, the intelligence rules, and the precise analysis of the pedestrian movement direction with surrounding neighbors. Then, our model can effectively avoid the pedestrian overlap and collision, and make the pedestrian simulation much more realistic and reliable. Meanwhile, the presented model is verified through multiple scenarios. We get the reliable fundamental diagram, the macroscopic phenomenon, and the pedestrian walking trajectory.

The remainder of this paper is organized as follows. In Section 2, we propose a new heuristic model based on the Voronoi diagram. We consider pedestrians' preference demand which affects the willingness to follow or detour others in heuristic rules. Then we propose many calculation principles and mechanisms for confirming the pedestrian walking direction. In Section 3, we discuss and analyze the simulation result in multiple scenarios. In Section 4, we conclude our work.

2. Heuristic model

2.1. Space and pedestrian

2.1.1. Voronoi diagram

Because of the Voronoi diagram's unique geometric characteristics, many scholars introduced the Voronoi diagram into pedestrian dynamics,[8,45–47] which is used to determine personal space, field, safety distance, and neighbors. Furthermore, pedestrians' local density and optimal velocity also can be obtained. Generally, the Voronoi diagram divides the two-dimensional space into irregular convex polygons according to particle sites. Among them, each particle is located in its polygonal region in which the particle has all the closest points. Then the polygon is defined as the Voronoi cell

(VC).[45,46] Moreover, the boundary of the Voronoi cell is defined as the Voronoi link (VL). The Voronoi link is shared by two adjacent Voronoi cells, which is the mid-perpendicular line between two adjacent particles. Meanwhile, the vertice of the Voronoi cell is defined as the Voronoi node (VN). Under the non-degenerate condition, the Voronoi node is associated with three Voronoi cells and is the intersection of three Voronoi links.

In the Voronoi diagram, pedestrians are regarded as particles and each Voronoi cell contains a pedestrian. Since each Voronoi cell contains all the areas in which the pedestrian can move access, the space of the Voronoi cell is considered as the possession of pedestrians.[8] Additionally, the shape of the Voronoi cell changes with the location of pedestrians in real-time. The Voronoi cell looks like a distorted cellular automaton but different from others because it has a unique irregular and non-empty cell. In particular, other pedestrians who share the same Voronoi link can be regarded as neighbors. The straight distance from the pedestrian to each Voronoi link can be regarded as a safe distance.

In the research of the combination of pedestrian dynamics with the Voronoi diagram, the region boundary has various forms.[8] In our studies, the Voronoi cell is cut off directly by the wall at the boundary. Then the original Voronoi link and the Voronoi node are replaced by the new corresponding ones automatically, as shown in Fig. 1.

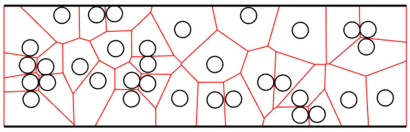


Fig. 1. The boundary form in the Voronoi diagram.

2.1.2. Pedestrian space

In our model, each pedestrian has a rigid and an elastic part and is represented by a two-layer circle, as shown in Fig. 2. The inner circle represents the rigid part of pedestrians, and the outer circle represents the elastic part of pedestrians. The elastic part deforms in real time with the pedestrian's velocity magnitude changes. Each part of pedestrians has a particular radius.

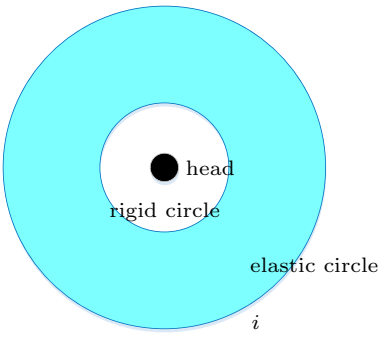


Fig. 2. The two-layer circle of pedestrian particle.

According to research data[47] and daily observation, the pedestrian's projection shape is close to an ellipse. In the traditional pedestrian simulation,[20] the pedestrian's elliptic projection shape is always represented as a circle. Moreover, their projected areas are basically equal. We can consider the original pedestrian's projection shape as an ellipse, as shown in Fig. 3(a). Then, by converting the pedestrian's elliptic area into a circular area, the rigid circle radius can be approximately obtained by

$$\pi \cdot (a_s/2) \cdot (b_s/2) = \pi \cdot r_s^2, \tag{1}$$

where a_s is the major axis length of the ellipse, b_s is the minor axis length of the ellipse, and r_s is the rigid circle radius.

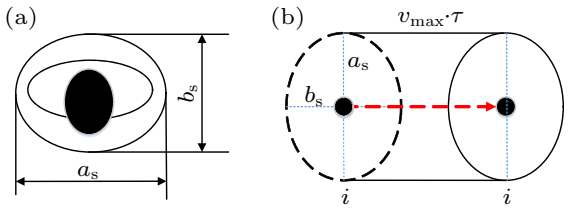


Fig. 3. Various shapes of different pedestrian space demands. (a) The shape in static pedestrian space demand; (b) the shape in dynamic pedestrian space demand.

When the pedestrian stands still, the shoulder width is the longest length of the pedestrian's projection area. If the shoulder width is taken as the pedestrian circle's diameter, pedestrians can get a relatively comfortable position and avoid touching the front and rear pedestrians. Then, half of the pedestrian's shoulder width can be used as the radius of the elastic circle when pedestrians stay stationary. In the empirical study,[20] the velocity magnitude of pedestrians in free flow, normal walk, and eager walk were 0.6 m/s, 1.0 m/s, and 1.5 m/s, respectively. The response time was 0.5 s. We regard the walking area of pedestrians as a rectangle area during the reaction time, as shown in Fig. 3(b). When pedestrians eagerly walk, by converting the sum of the pedestrian's projection area and the pedestrian's walking area into a circular area, the elastic circle radius can be approximately obtained by

$$\pi \cdot (a_s/2) \cdot (b_s/2) + v_{max} \cdot \tau \cdot a_s = \pi \cdot r_{max}^2, \tag{2}$$

where τ is the relaxation time, v_{max} is regarded as the maximum walking velocity magnitude, and r_{max} is the elastic circle radius.

Pedestrians need various dynamic space sizes in suitable velocity magnitude. Generally, the higher the velocity magnitude, the larger the dynamic space area. As a linear relationship between the velocity magnitude and the dynamic elastic circle radius, the calculation formula is shown in Eq. (3). For example, when the velocity magnitude is zero, the dynamic elastic circle radius approximately equals the rigid circle radius. And when the velocity magnitude is maximum, the dynamic elastic circle radius equals the largest limiting radius.

$$r_e = (r_{max} - r_0)/v_{max} \cdot v_e + r_0, \tag{3}$$

where v_e is the instant velocity magnitude, r_e is the dynamic elastic circle radius, and r_0 is the static elastic circle radius.

According to geometric characteristics of the Voronoi diagram,[8] the definition of the local density is the ratio of the number of pedestrians to the area of the Voronoi cell. The calculation is shown in Eq. (4). The local density can be divided into four thresholds of low density (1 p/m^2), medium density (1 p/m^2–2.5 p/m^2), medium-high density (2.5 p/m^2–5 p/m^2), and high density (5 p/m^2).[8]

$$\rho = 1/s_1, \tag{4}$$

where ρ is the local density of pedestrians, s_1 is the area of the pedestrian's Voronoi cell.

The effective area ratio of pedestrians is the ratio of the area of the dynamic elastic circle to the area of the Voronoi cell. According to the instant elastic circle radius of each pedestrian, the area of each pedestrian's dynamic elastic circle can be obtained, as shown in Eq. (5). Then, the effective area ratio of each pedestrian can be obtained, as shown in Eq (6).

$$s_0 = \pi \cdot r_e^2, \tag{5}$$

$$\gamma = s_0/s_1, \tag{6}$$

where, s_0 is the area of the dynamic elastic circle of pedestrians, and γ is the effective area ratio of pedestrians.

Furthermore, we can see the state of crowded pedestrians changes with the change of the effective area ratio γ. Moreover, the situation of $\gamma < 1$ or $\gamma > 1$, which means the pedestrian is in a normal non-crowded state or a crowded state, respectively, as shown in Fig. 4. In our research, we focus on the non-crowded state of $\gamma < 1$ in the whole paper.

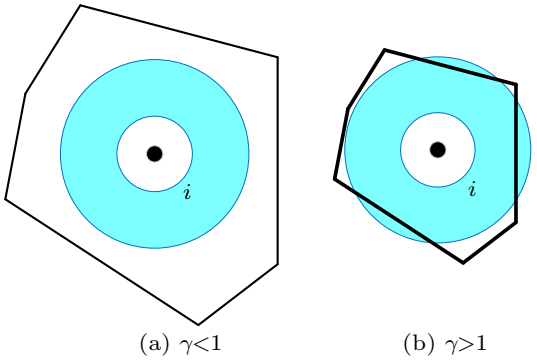


Fig. 4. The characteristics of pedestrians with different effective area ratios. (a) The non-crowded state of $\gamma < 1$; (b) the crowded state of $\gamma > 1$.

We might observe a scene where two pedestrians are particularly close. The pedestrians' dynamic elastic parts and rigid parts show the situation of cross and separate, respectively. Although pedestrians are crowded, they are still within the tolerance range, as shown in Fig. 5. However, if the pedestrians' rigid parts intersect, they usually get injured beyond the tolerance range.

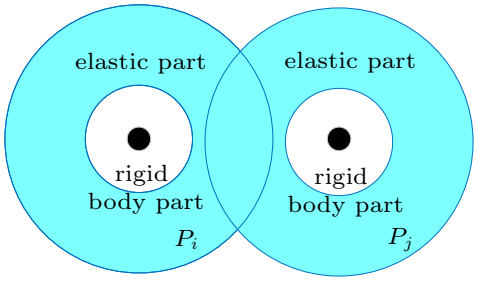


Fig. 5. The scene of two pedestrians intersect.

2.2. Detour behaviors

Generally, pedestrians detour or follow others can be seen everywhere in daily life. For example, when a healthy young adult is taking a walk and a slow-walking older adult or a stationary obstacle ahead, the young adult would speed up to detour. When two normal pedestrians walk in the opposite direction, at least one pedestrian could notice the oncoming pedestrian and change the movement direction in advance instead of insisting on the original movement direction and colliding with the other pedestrian. When a group of rush pedestrians on the subway platform, though most pedestrians could reduce the detour behavior and follow others in front, the other pedestrians might eagerly choose to go through the limited gap.

In the simulation, though the traditional SFM can excellently reproduce most of the self-organizing phenomena, some unreasonable congestions or deadlocks still occur.[36,45] The pedestrian desired direction is simply set to the destination and is not dynamically updated. In Fig. 6, two pedestrians are located at the up and the down center of the corridor in a line, respectively. The destination of pedestrian i and pedestrian j is the up end of the corridor. If simply setting the desired direction (0, 1) for pedestrian i and pedestrian j, they are walking in the same direction and the rear pedestrian walks fast, as shown in Fig. 6(a). Or the destination of pedestrian i is the up end and pedestrian j is the down end of the corridor. If simply setting the desired direction (0, 1) for pedestrian i and (0, -1) for pedestrian j, they are walking in the opposite direction, as shown in Figs. 6(b) and 6(c). The resulting force of pedestrians might finally cause a collision between them and even lead to an unreasonable deadlock. For example, pedestrians are located at the final conflicting locations i_1 and j_1, respectively, as shown in Fig. 6(b). However, in reality, at least one pedestrian might change the walking direction and choose to detour instead of insisting on the original direction. For example, pedestrians are located at the final non-conflict locations i_2 and j_1 respectively, as shown in Fig. 6(b).

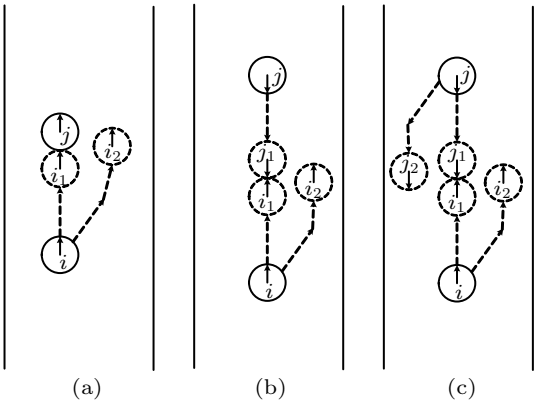


Fig. 6. Some unreasonable situations occur in the traditional SFM. (a) Pedestrian i and pedestrian j, walking in the same direction. In the simulation of the traditional SFM, pedestrian i would move to location i_1, but in reality, *e.g.*, the final location might be i_2; (b) pedestrian i and pedestrian j are walking opposite to each other. In the simulation of the traditional SFM, pedestrian i and pedestrian j would move to location i_1 and location j_1, respectively, but in reality, *e.g.*, pedestrian i might move to location i_2 and pedestrian j might move to location j_1 along the original direction; (c) opposing the movement of pedestrian i and pedestrian j, in the simulation of the traditional SFM, pedestrian i and pedestrian j would move to the location i_1 and location j_1, respectively but in reality, *e.g.*, both the pedestrian i and pedestrian j might move respectively to location i_2 and location j_2.

2.3. Heuristic rules

The traditional heuristics mainly determine the pedestrian velocity direction and magnitude according to two heuristic rules of the demand of pedestrians walking quickly and safely.[8,37] In our model, we propose a third movement demand of pedestrians' preference and willingness.

In general, pedestrians expect to reach the destination in the shortest time. Obviously, the velocity direction directly point to the destination is the most popular choice of pedestrians. However, obstacles and other slow-speed pedestrians might be located in the shortest movement direction of the normal walking pedestrian, which may induce the motion conflict.

Therefore, pedestrians need to balance the collision avoidance and minimize the detour distance and choose the optimal velocity direction. Meanwhile, pedestrians usually need specific buffer time to evade other obstacles or neighbors and compensate for the delay to maintain sufficient safety distance and adjust reasonable velocity magnitude.

However, pedestrians are intelligent in the actual walking process. Many certain and uncertain factors can determine their behaviors. Pedestrians not only need to consider the demand for walking fast and safe but also need to consider many other factors. Such as age, gender, habits, mood, companions, neighbors, environments, travel purpose, and travel time. Even the same pedestrian might choose various movement behavior under the same environmental condition at a different time. We also can see the unusual phenomenon that pedestrians choose to detour quickly or follow others though the scenarios are not suitable or they can make other reasonable choices. For example, some older adults or young girls prefer to follow others or stroll with peers instead of walking fast. Then, based on the two traditional heuristic rules above, we propose a third movement demand of pedestrians' preference and willingness.

Since pedestrians' preference and willingness demand are composed and influenced by many factors, we simplify the process and unify the demand into pedestrians' detour or follow behavior choice. We consider the preference and willingness demand can affect pedestrians' behavioral determination. For example, pedestrians intend to detour and could when the external condition is appropriate for a detour. Furthermore, pedestrians do not intend to detour and could choose to follow, though the external condition is still appropriate for a detour.

Meanwhile, for pedestrians' safe walk demand, we also propose an anti-deadlock mechanism to prevent conflicts in the counter-directional pedestrian flow. When walking in the opposite direction, adjacent pedestrians might involuntarily choose to detour each other. The situation may cause a new conflict which leads to unreasonable congestion and deadlock. In order to avoid such unreasonable phenomenon, we set a rule that pedestrians must make reasonable velocity direction choice based on the local density. Besides, for pedestrians' fast and comfortable walk demand, we propose a site-fine-tuning mechanism that pedestrians' locations would be fine-tuned to avoid pedestrians getting too close to neighbors.

2.4. Elementary characteristics of velocity direction

The pedestrian movement can be divided into two stages of cognition and action.[8] In the stage of cognition, the movement information is identified, such as location, velocity, local density, neighbors, and safety distance. In the stage of action, based on the existing cognitive information, the velocity direction and magnitude of pedestrians are decided. According to the heuristic rules, the pedestrian movement choice is mainly based on the demand for fast, safe, preferences, and willingness. By using the geometric characteristics of the Voronoi diagram, we can obtain pedestrians' personal domain, which includes local density, safety distance, and neighbors. We consider that the elementary characteristics of the velocity direction should include the target/follow direction and the detour direction, as shown in Fig. 7. Especially, we think that pedestrians mainly choose to follow others in the target direction.

The target/follow direction is a unit direction vector from the pedestrian center to the target point. According to the demand for walking fast and preference, pedestrians like directly walking to the target point instead of deviating from it. The target/follow direction is the primary choice as the velocity direction of pedestrians. The calculation of the target/follow direction e^{des} is shown as

$$e^{\text{des}} = (D_i - P)/(||D_i - P_i||), \tag{7}$$

where P_i and D_i represent pedestrians' location coordinate and target point, respectively.

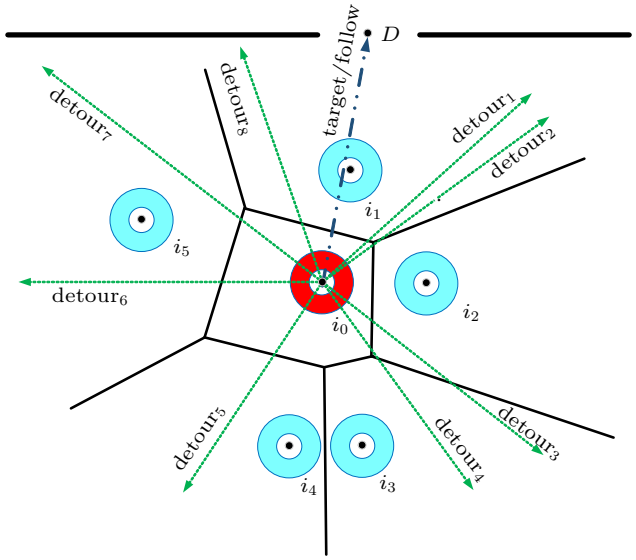


Fig. 7. The basic characteristics of the velocity direction. The blue arrow is the target/follow direction, and the green arrows are various potential detour directions.

The detour direction is a unit direction vector from the pedestrian center to both sides of others in which pedestrians can detour successfully. According to the demand for walking safely and preference, pedestrians could detour others. The calculation of the detour direction $\boldsymbol{e}^{\text{detour}}$ is shown as

$$\boldsymbol{e}^{\text{detour}} = (n_i - P)/(||n_i - P_i||), \tag{8}$$

where P_i represents pedestrians' coordinate, and n_i represents the intersection point of the detour direction with the corresponding Voronoi link.

2.5. Determination of walking direction

Based on the situation of the existing space and the movement preference, pedestrians make decisions to follow or detour others. When deciding to detour, pedestrians not only need to consider the relationship with neighbors, but also need to consider the relationship with obstacles and walls. Then we can obtain a set of possible detour directions for pedestrians to decide, and we need to choose the optimal detour direction. The decision process of the optimal movement direction for pedestrians to choose is shown in Fig. 8.

2.5.1. Choice of walking direction

In the simulation when facing surrounding complex environments pedestrians should decide the movement behavior of detour or follow others to avoid potential collisions. For example, when walking in the original target direction, if pedestrians are going to collide with others, they should instantly choose the temporary direction to detour or follow. The target direction $\boldsymbol{e}^{\text{dir}}$ choice process could be clearly identified as

$$\boldsymbol{e}^{\text{dir}} = \begin{cases} \boldsymbol{e}^{\text{detour}}, & \text{if } d_{ij} - \boldsymbol{\tau} \cdot (\boldsymbol{v}_i - \boldsymbol{v}_j) \cdot \boldsymbol{e}_{ij} < r_i + r_j + \varepsilon, \\ \boldsymbol{e}^{\text{des}}, & \text{otherwise}, \end{cases} \tag{9}$$

where $\boldsymbol{e}^{\text{detour}}$ is the detour direction, $\boldsymbol{e}^{\text{des}}$ is the original target direction, $\boldsymbol{e}_{ij}$ is the unit vector pointing from pedestrian i to pedestrian j, d_{ij} is the distance between pedestrian i and pedestrian j, τ is the relaxation time, ε is a parameter that controls the safe distance between pedestrians, r_i and r_j are the radius of pedestrian i and pedestrian j, respectively. Especially, $\boldsymbol{v}_i$ and $\boldsymbol{v}_j$ indicate the normal walking velocity of pedestrian i and pedestrian j in the original target direction respectively.

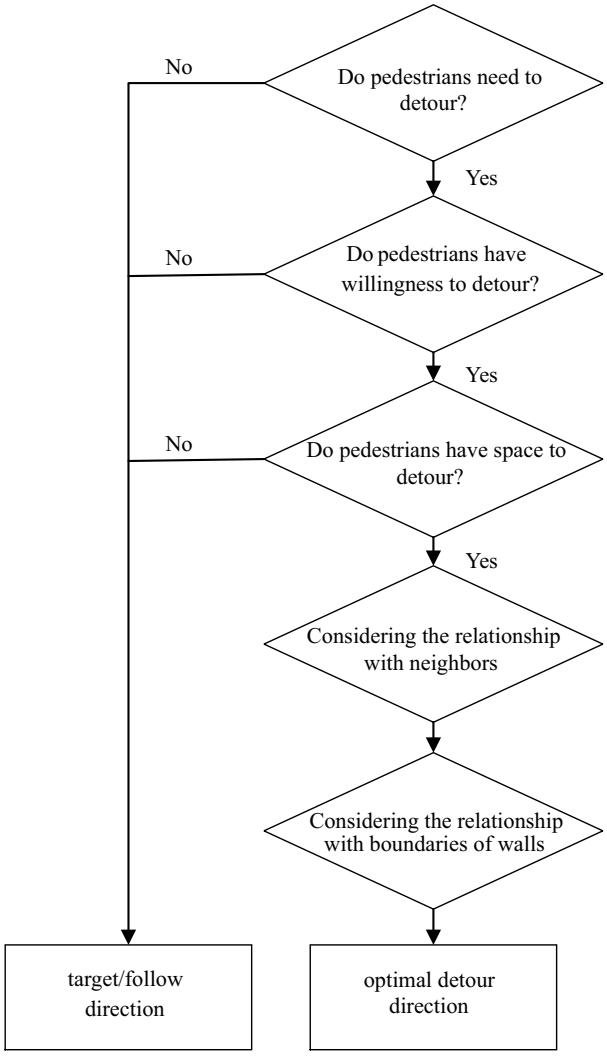


Fig. 8. The decision-making process of pedestrians' movement direction.

2.5.2. Calculation principle of detour direction

Since pedestrians have the demand to detour others, we propose principles to calculate the exact detour direction. We assume that the red detouring-pedestrian i_0 could detour both sides of the surrounding blue detoured-pedestrian i_1 at the minimum angle. Especially, we set a pair of virtual yellow pedestrian i_1' and pedestrian i_1'' which tangent with both sides of the blue detoured-pedestrian i_1 respectively. The hypothetical situation is shown in Fig. 9. Then, we set both of the center coordinates of the yellow virtual pedestrians are O_1' (x_1, y_1) and O_1'' (x_2, y_2), respectively. Moreover, we also unify them as (x, y) in Eq. (10) for convenience, and we can obtain them

from Eqs. (10)–(12).

$$
\begin{aligned}
& l_{O_1O_1'(O_1O_1'')} \\
&= ||O_1'(O_1'') - O_1|| = \sqrt{(x-x_{O_1})^2 + (y-y_{O_1})^2}, \\
& l_{O_1O_1'(O_1O_1'')} = r_{i_0} + r_{i_1} + \alpha, \qquad (10) \\
& l_{O_1O_0} \\
&= ||O_0 - O_1|| = \sqrt{(x_{O_0}-x_{O_1})^2 + (y_{O_0}-y_{O_1})^2}, \qquad (11) \\
& l_{O_1O_1'(O_1O_1'')}/l_{O_1O_0} \\
&= (\boldsymbol{l}_{O_1O_1'(O_1O_1'')} \cdot \boldsymbol{l}_{O_1O_0})/(l_{O_1O_1'(O_1O_1'')} \cdot l_{O_1O_0}), \qquad (12)
\end{aligned}
$$

where, (x_{O_0}, y_{O_0}) is the center coordinate of the red detouring-pedestrian i_0, (x_{O_1}, y_{O_1}) is the center coordinate of the blue detoured-pedestrian i_1, and α is a parameter that controls the distance between the detoured-pedestrian and the detouring-pedestrian.

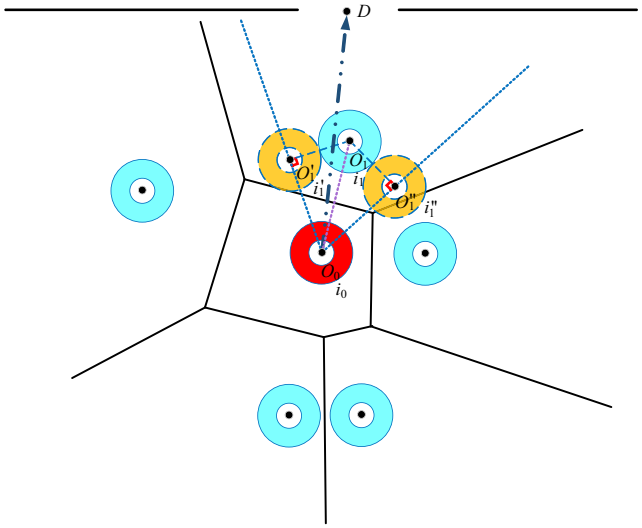


Fig. 9. The situation of the detouring-pedestrian intends to detour one major neighbor. The red circle represents the detouring-pedestrian i_0, the major blue circle ahead represents the detoured-pedestrian i_1, and the yellow circles represent the pair of virtual pedestrian i_1' and pedestrian i_1''.

After the pair of the virtual pedestrians' center coordinates obtained, we can get both of the available detour directions of the detouring-pedestrian as

$$
\boldsymbol{e}^{\text{detour}} = \begin{cases} (O_1' - O_0)/(||O_1' - O_0||), \\ (O_1'' - O_0)/(||O_1'' - O_0||). \end{cases} \qquad (13)
$$

2.5.3. Relationship with neighbors

Generally speaking, pedestrians usually have multiple neighbors, so we should judge whether the pedestrian can pass through every two adjacent neighbors. We assume that both of the blue detoured-pedestrian i_1 and detoured-pedestrian i_5 in front of the red detouring-pedestrian i_0, as shown in Fig. 10. Obviously, the center coordinates of the corresponding two pairs of the yellow virtual pedestrians can be obtained from Eqs. (10)–(13). Next, we should judge which two virtual pedestrians are sandwiched between the detoured-pedestrian i_1 and detoured-pedestrian i_5. The way to calculate the center coordinates of the two sandwiched virtual pedestrians can be obtained as

$$
n_{\text{inner1}} = \begin{cases} O_1', \text{ if } \angle O_1'O_0O_5 < \angle O_1''O_0O_5, \\ O_1'', \text{ if } \angle O_1'O_0O_5 > \angle O_1''O_0O_5, \end{cases} \qquad (14)
$$

$$
n_{\text{inner5}} = \begin{cases} O_5', \text{ if } \angle O_5'O_0O_1 < \angle O_5''O_0O_1, \\ O_5'', \text{ if } \angle O_5'O_0O_1 > \angle O_5''O_0O_1, \end{cases} \qquad (15)
$$

where n_{inner1} and n_{inner5} are the center points of the two sandwiched virtual pedestrians.

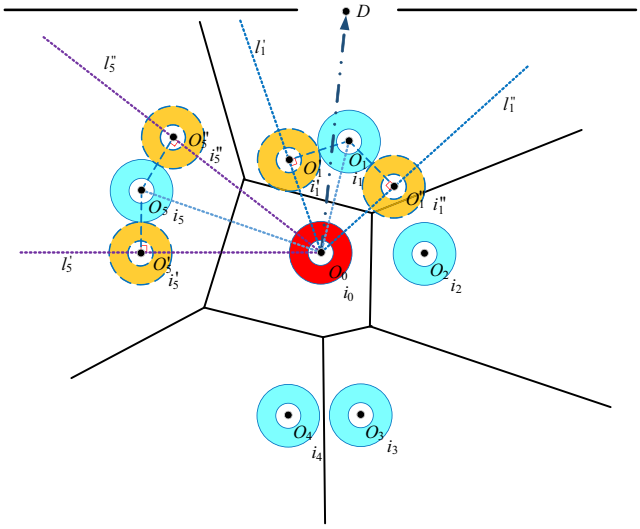


Fig. 10. The situation of the detouring-pedestrian can pass through two adjacent neighbors.

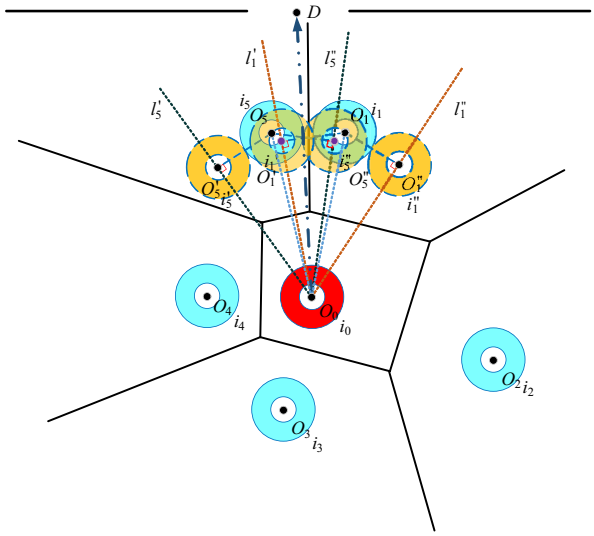


Fig. 11. The situation of the detouring-pedestrian cannot pass through two adjacent neighbors.

By judging the relative location relationship with the center coordinates of the two sandwiched virtual pedestrians and the two detoured-pedestrians, we can judge whether the detouring-pedestrian can pass through the two detoured-pedestrians. We set O_1' and O_5'' are the center points of the two sandwiched virtual pedestrians. If $\angle O_1'O_0O_1 < \angle O_5''O_0O_1$ the red detouring-pedestrian i_0 can pass through the blue detoured-pedestrian i_1 and detoured-pedestrian i_5 as shown

in the case of Fig. 10. If $\angle O_1' O_0 O_1 > \angle O_5'' O_0 O_1$, the red detouring-pedestrian i_0 cannot pass through the blue detoured-pedestrian i_1 and detoured-pedestrian i_5, as shown in the case of Fig. 11. Meanwhile, the two detour directions $\boldsymbol{O_0 n}_{\text{inner1}}$ and $\boldsymbol{O_0 n}_{\text{inner2}}$ are not in the selection set of available detour directions of the detouring-pedestrian i_0.

2.5.4. Relationship with boundaries

In addition to the relationship with neighbors, pedestrians also need to consider the relationship with the wall. We assume that the red detouring-pedestrian i_0 closes to the wall W_1 and the distance between them is d_0, as shown in Fig. 12(a). Then, we get both of the potential detour directions that the red detouring-pedestrian i_0 bypasses the blue detoured-pedestrian i_1 by Eqs. (10)–(13). And we set the detour directions as $\boldsymbol{l}_1'$ and $\boldsymbol{l}_1''$, respectively. Obviously, the detour direction $\boldsymbol{l}_1''$ of the detouring-pedestrian i_0 points to the wall W_1, and the detouring-pedestrian i_0 would collide with the wall W_1 if choosing the movement direction $\boldsymbol{l}_1''$. But this situation does not fit the common sense. Therefore, we set that when the distance d_0 between the pedestrian and wall fits $d_0 < \beta$, the detour direction that points to the side of the wall is not in the selection set of the available detour direction. Where, β is a parameter that controls whether the distance d_0 can affect the choice of the pedestrian detour direction. By contrast, when $d_0 > \beta$ the detouring-pedestrian i_0 is away from the wall W_1 (see Fig. 12(b)), and then both of the potential directions are in the set of the available detour directions of the pedestrian i_0.

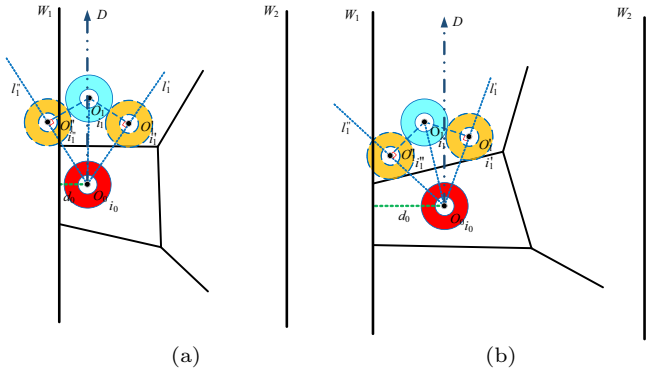


Fig. 12. The relationship between the pedestrian and the wall. (a) The situation of $d_0 < \beta$ that the detouring-pedestrian could not choose the direction to the wall; (b) the situation of $d_0 > \beta$ that the detouring-pedestrian could choose the direction to the wall.

2.5.5. "Allow-areas and denial-areas" for walking direction choice

Considering pedestrians usually facing multiple neighbors at the same time, we propose a pair of "allow-areas and denial-areas" rule to screen the set of the available detour direction of the detouring-pedestrian. We assume that the red detouring-pedestrian i_0 is surrounded by five blue neighbor-pedestrians i_1, i_2, i_3, i_4, and i_5, as shown in Fig. 13. With the detouring-pedestrian i_0 and the detoured-pedestrian i_1, we set both of the center points of the yellow virtual pedestrians are O_1', O_1'', respectively. Besides, the critical detour direction $\boldsymbol{O_0 O_1'}(\boldsymbol{l}_1')$ satisfies $\boldsymbol{O_1 O_1'} \perp \boldsymbol{O_0 O_1'}$. Similarly, the critical detour direction $\boldsymbol{O_0 O_1''}(\boldsymbol{l}_1'')$ satisfies $\boldsymbol{O_1 O_1''} \perp \boldsymbol{O_0 O_1''}$. Then the detouring-pedestrian i_0 can judge the surrounding situation once with the detoured-pedestrian i_1. No matter which movement direction is chosen for pedestrian i_0 walking into the area $l_1' O_0 l_1''$, the detouring-pedestrian i_0 would collide with the detoured-pedestrian i_1. Then this area $l_1' O_0 l_1''$ is marked as "denial-areas" which is a collision area between the detouring-pedestrian i_1 and the detoured-pedestrian i_0. Meanwhile, the detouring-pedestrian i_0 would not collide with the detoured-pedestrian i_1 when walking outside the area $l_1' O_0 l_1''$. Then the area that outside $l_1' O_0 l_1''$ is marked as "allow-areas," which is an accessible area between the detouring-pedestrian i_1 and the detoured-pedestrian i_0. Especially, the detouring-pedestrian i_0 needs to judge and select all the "allow-areas" and "denial-areas" with the other neighbors. Obviously, we can get the final "allow-areas" of the detouring-pedestrian i_0 based on whether the detouring-pedestrian i_0 can smoothly walk without any collisions, and the final "denial-areas" are out of the final "allow-areas" in which the detouring-pedestrian i_0 could collide with any of the neighbors.

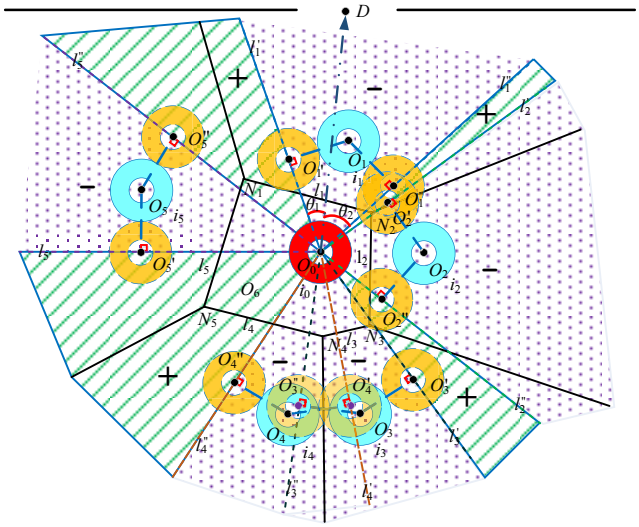


Fig. 13. The situation that the detouring-pedestrian has many "allow-areas" and "denial-areas". The areas with many plus signs mean the final "allow-areas" and the areas with many minus signs mean the final "denial-areas" of the detouring-pedestrian.

In summary, for the detouring-pedestrian, we set that area T_{region0} equals area T_{region1} intersecting area T_{region2},

$$T_{\text{region0}} = T_{\text{region1}} \cap T_{\text{region2}}. \tag{16}$$

Moreover, we set that the area has two properties of "allow-areas" or "denial-areas." The plus sign means the property of the area is "allow-areas" and the minus sign means the

property of the area is "denial-areas." According to Eq (16), if we want to judge the property of area T_{region0} we need to see both of the properties of area T_{region1} and area T_{region2}. The judgment method of the property of area T_{region0} as shown in Eq. (17).

$$T_{\text{region0}} = \begin{cases} T_{\text{region0}}(+), \text{ if } T_{\text{region1}}(+) \cap T_{\text{region2}}(+), \\ T_{\text{region0}}(-), \text{ if } T_{\text{region1}}(+) \cap T_{\text{region2}}(-), \\ T_{\text{region0}}(-), \text{ if } T_{\text{region1}}(+) \cap T_{\text{region2}}(-). \end{cases} \quad (17)$$

As mentioned above, we have got the "allow-areas" and "denial-areas" of the detouring-pedestrian. Next, we need to find the optimal movement direction of the detouring-pedestrian. If the target direction in the "allow-areas," then the detouring-pedestrian could choose this direction to move. If the target direction in the "denial-areas," then we have two different situations to consider. When the detouring-pedestrian has many "allow-areas" and "denial-areas," we choose the movement direction with the smallest deviation angle from the target direction in the "allow-areas." The detouring-pedestrian prefers to seek the shortest distance to the destination. For example, due to $\theta_1 < \theta_2$, we choose the movement direction l_1' instead of l_1'', as shown in Fig. 13. By contrast, when the detouring-pedestrian only has many "denial-areas," we have to choose the target direction to follow with the limited velocity magnitude, because the detouring-pedestrian is forced to slow down or even standstill. We can see the example in the following Fig. 14.

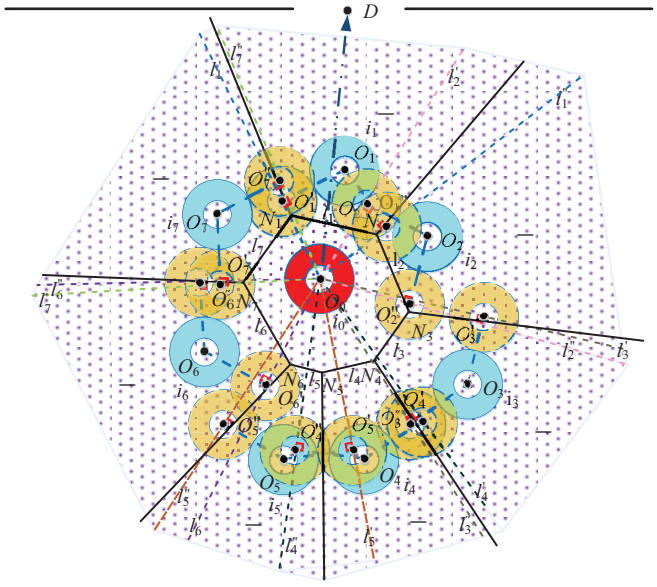


Fig. 14. The situation that the detouring-pedestrian only has many "denial-areas." The areas with many minus signs mean the final "denial-areas" of the detouring-pedestrian.

2.6. A microscopic anti-deadlock mechanism

In the process of avoiding collision between the adjacent pedestrians in the counter-directional flow, sometimes we could see the unreasonable phenomenon of the new collision occurrence and even deadlock in the simulation, as shown in Fig. 15(a). The effect of the anti-deadlock mechanism is related to the scale of the pedestrian, the simulation scene and the movement preference. We focus on the microscale anti-deadlock mechanism in our paper. In order to avoid the unreasonable phenomenon, we set a microscopic anti-deadlock mechanism. When adjacent pedestrians walk in the opposite direction, the pedestrian with low local density could choose the optimal detour direction because he/she has much more space but the other pedestrian with high local density has to choose the original target direction or standstill, as shown in Fig. 15(b).

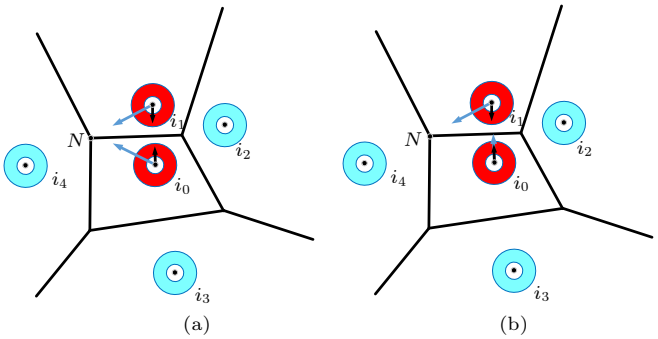


Fig. 15. The situation that the adjacent pedestrians in the counter-directional flow. The black arrow indicates the original target direction, and the blue arrow indicates the detour direction. (a) The situation that a new collision would occur when pedestrians detour spontaneously; (b) the situation that the collision would avoid when pedestrians move rationally.

2.7. Determination of velocity

When walking to the boundary of the Voronoi cell along the movement direction, pedestrians need to ensure the essential safe distance during the reaction time. Moreover,

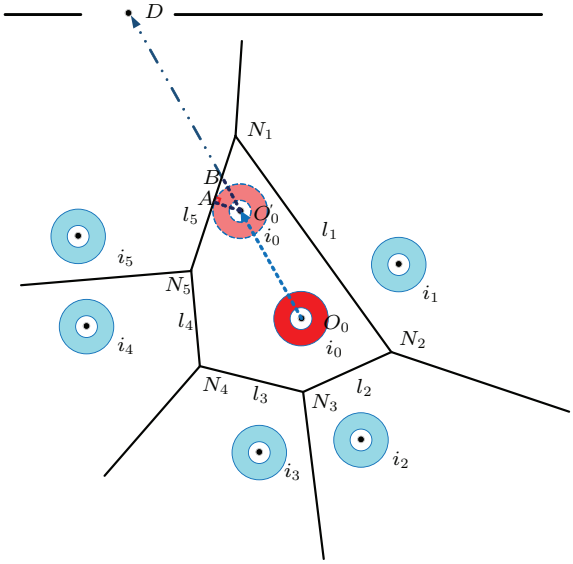


Fig. 16. The pedestrian movement in the Voronoi cell during the reaction time. The dark red circle indicates that the detouring-pedestrian in the original location before walking, and the light red circle indicates that the detouring-pedestrian in the expected location after walking during the reaction time.

the pedestrians wish to move as far as possible to the location in which could tangent with the corresponding Voronoi link, as shown in Fig. 16. Then the calculation methods for the expected velocity magnitude v_0 and the acceleration $\boldsymbol{a}_0$ are shown in Eqs. (18)–(19).

$$v_{\rm o} = \begin{cases} v_{\max}, & \text{if } l_{\max} \le l_{O_0O'_0}, \\ l_{O_0O'_0}/\tau, & \text{otherwise}, \end{cases} \tag{18}$$

$$\boldsymbol{a}_{\rm o} = ((\boldsymbol{v}_0 - \boldsymbol{v}'_0)\cdot \boldsymbol{n}_0)/\tau, \tag{19}$$

where τ is the relaxation time $v_{\max}$ is the maximum walking velocity magnitude, $l_{\max}$ is the distance when pedestrians walking at the maximum velocity magnitude during the relaxation time, $\boldsymbol{n}_0$ is the walking direction, $l_{O_0O'_0}$ is the distance along the walking direction to the location where pedestrians could tangent with the Voronoi link, and v'_0 is the current velocity magnitude.

2.8. A site-fine-tuning mechanism

Generally, pedestrians pursue the comfort of their personal space. Then, we propose a site-fine-tuning mechanism to avoid pedestrians from getting too close to neighbors. From the linear relationship between the velocity magnitude and the radius of the elasticity circle in Eq. (3), we can get the instant dynamic elastic circle radius. Pedestrians usually want to move at higher velocity magnitude within the safe distance, which causes pedestrians to tangent with or close to the corresponding Voronoi link. However, at this time, the pedestrian's invisible dynamic elastic circle might intersect with the Voronoi link, as shown in Fig. 17.

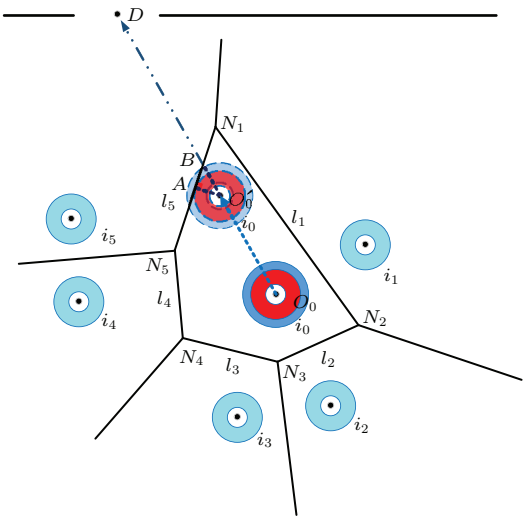


Fig. 17. The detouring-pedestrian's invisible dynamic elastic circle intersects with the Voronoi link. The red circle represents the static elastic circle, and the blue circle represents the dynamic elastic circle.

The adjustment range of the pedestrian's site-fine-tuning is that the vector sum of the walking distance of the pedestrians' dynamic elastic circle with the intersection of the Voronoi links. The reverse movement direction is from the intersection of the Voronoi links to the pedestrian center until the dynamic elastic circle does not intersect with each Voronoi link as much as possible. For example, since the intersection between the pedestrian and the Voronoi links, the pedestrian needs to make a site-fine-tuning as shown in Fig. 18(a). After the site-fine-tuning, the pedestrian does not intersect with each Voronoi link again as shown in Fig. 18(b). The calculation of the pedestrian's site-fine-tuning $\boldsymbol{l}_{\rm finetune}$ is shown in Eq. (20).

$$\boldsymbol{l}_{\rm finetune} = l_{\rm A_1B_1}\cdot \boldsymbol{n}_{\rm A_1O_0} + l_{\rm A_4B_4}\cdot \boldsymbol{n}_{\rm A_4O_0} + \cdots, \tag{20}$$

where, $\boldsymbol{n}_{\rm A_1O_0}$, $\boldsymbol{n}_{\rm A_4O_0}$, *etc.* are unit vectors of the site-fine-tuning in each direction reverse to the Voronoi links, and $l_{\rm A_1B_1}$, $l_{\rm A_4B_4}$, *etc.* are the fine-tuning distances in each direction reverse to the Voronoi links.

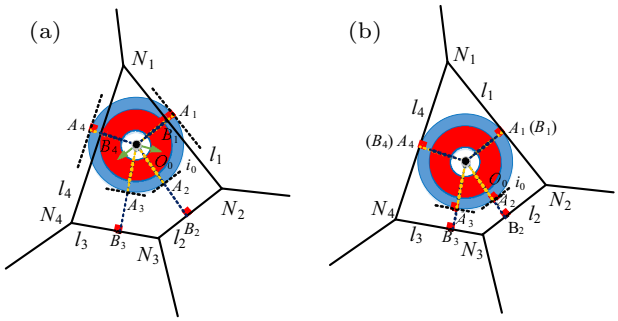


Fig. 18. The site-fine-tuning mechanism of pedestrians. The red circle represents the static elastic circle, and the blue circle represents the dynamic elastic circle of the detouring-pedestrian.

2.9. Update rules

In this paper, we focus on the non-crowded state. The pedestrians' location and velocity can be updated as shown in Eqs. (21)–(23). Where, $\boldsymbol{a}_i$ is the acceleration, $\boldsymbol{v}_i$ is the velocity, $\boldsymbol{x}_i$ is the location, and Δt is the simulation time interval.

$$\boldsymbol{a}_i = {\rm d}\boldsymbol{v}_i/{\rm d}t, \tag{21}$$

$$\boldsymbol{x}_i(t+\Delta t) = \boldsymbol{x}_i(t) + \boldsymbol{v}_i(t)\cdot\Delta t + (1/2)\cdot\boldsymbol{a}_i(t)\cdot(\Delta t)^2, \tag{22}$$

$$\boldsymbol{v}_i(t+\Delta t) = \boldsymbol{v}_i(t) + \boldsymbol{a}_i(t)\cdot\Delta t. \tag{23}$$

3. Simulations and analyses

This section, we simulate and analyze the pedestrian flow to verify the reliability of this model in different scenarios. The scenarios include unidirectional pedestrian flow, bidirectional pedestrian flow, with static obstacles in the corridor, and evacuation from a room with single exit. In order to clearly distinguish the local density of each pedestrian in real time, the Voronoi cells are filled with different colors according to the local density of pedestrians. The Voronoi cell filled with green, yellow, orange, and red indicates low density, medium density, medium high density, and high density, respectively. During the simulation process, the color of the Voronoi cell can be used to observe the crowdedness of pedestrians at different location and time. Besides, the shape and the color of

the Voronoi cells change with the change of the pedestrians' location and density in real time. We set $\tau = 0.5$ s, $\Delta t = 0.1$ s, $r_0 = 0.3$ m, $v_0 = 1$ m/s, $v_m = 1.5$ m/s, and $\alpha = 0$ which means the detouring-pedestrian just detour the detoured-pedestrian with the minimum distance.

3.1. A corridor with unidirectional flow

The simulation of unidirectional pedestrian flow is carried out in a long straight corridor of 10 m × 3 m with periodic boundaries, as shown in Fig. 19. The pedestrians enter the corridor from lower side and leave from upper side, and then re-enter the corridor again and again. The number and the overall density of pedestrians are always fixed in the process. In the beginning, pedestrians are randomly distributed in the corridor, and the local density of each pedestrian is different, as shown in Fig. 19(a). Subsequently, a trend of uniform distribution as the move of pedestrians can be seen in Fig. 19(b). Finally, we can see four queues of pedestrians in the corridor of 3-m-wide. Especially, we can see the pedestrians are basically evenly distributed. Meanwhile, the velocity magnitude of each pedestrian is approximately equal, and the local density of pedestrians is almost the same in the Voronoi cell, as shown in Fig. 19(c).

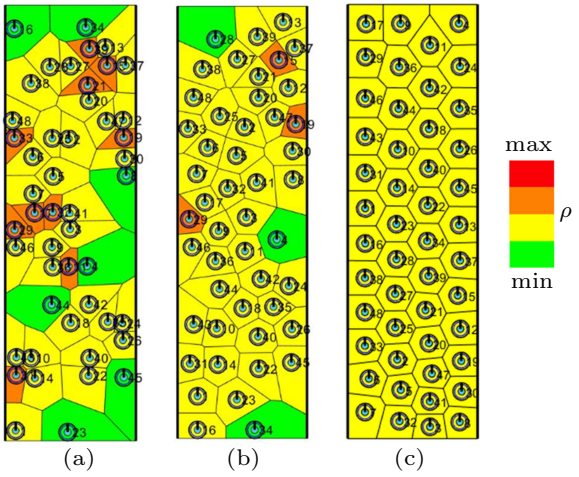


Fig. 19. The simulation snapshots of unidirectional pedestrian flow in the corridor. There are 48 pedestrians move from lower side to upper side in the 10 m × 3 m corridor. The pedestrians are represented by the circle, and the Voronoi cells corresponding to the pedestrians are filled with the color based on the local density of pedestrians.

In order to obtain the velocity–density relationship in unidirectional flow, we simulate the pedestrian movement under different overall density conditions (0.2 p/m^2–5 p/m^2). However, due to pedestrian flow with high-density (> 5 p/m^2) is not the focus of this paper, we do not simulate pedestrian movement under the very high density condition. In the simulation with different overall density, pedestrians are initially and randomly distributed in the corridor, and their movement destinations are located at the upper end of the corridor. Each simulation experiment repeats 10 times and lasts 90 simulation time steps. The initial 30 simulation time steps are warm-up time, and the data of the next 60 simulation time steps would be used for statistical analysis. We compare our velocity–density relationship data with actual data[48–52] and other heuristic simulation data[8] in Fig. 20. We can see that our data is in good agreement with the empirical data and other heuristic simulation data in the fundamental diagram. Besides, by comparing with the other heuristic simulation data,[8] maybe because the rules of this paper optimize the velocity direction choice of pedestrians, the pedestrian flow has a relatively higher walking velocity magnitude, and the free-flow phase of pedestrians covers at 0 p/m^2–1.1 p/m^2.

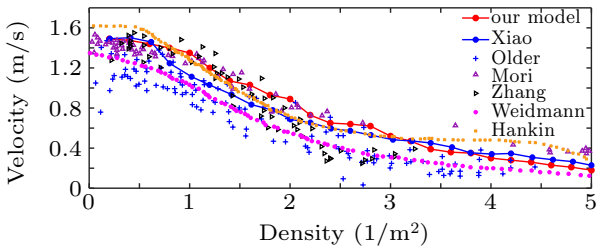


Fig. 20. The fundamental diagram of unidirectional pedestrian flow in the corridor (0 p/m^2–5 p/m^2). Actual data (Older,[48] Mori,[49] Zhang,[50] Weidmann,[51] Hankin,[52]) and heuristics simulation data (Xiao,[8]) are gathered to compare with our model.

3.2. A corridor with bidirectional flow

In a 7 m × 2.5 m corridor the simulation of bidirectional pedestrian flow with periodic boundaries is performed. The pedestrians would re-enter the corridor from the other side after leaving the system. Eight pedestrians are randomly distributed initially, of which four pedestrians (with black vertical lines) move from bottom to top of the corridor and the other four pedestrians (with red vertical lines) move from top to bottom of the corridor as shown in Fig. 21(a). In order to avoid collisions, the pedestrians would always spontaneously fine-tune their walking directions in the counter flow, or follow the previous pedestrians in the same direction, as shown in Figs. 21(b) and 21(c). Then the behaviors of pedestrians lead to the separation of counter pedestrian flow and the formation of pedestrian movement lanes. Besides, pedestrians can even retreat during the progress. When the simulation is stable, we can see that the pedestrians of the same direction following the others in front of them and three walking lanes are formed with the opposite direction, as shown in Fig. 21(d). During the process, we can see the anti-deadlock and detour behaviors of pedestrians clearly and then observe about four times of micro-scale anti-deadlock behaviors before forming a steady flow in Fig. 21.

Especially, the rapid transition of bidirectional flow from disorder to order is impressively demonstrated by Yamori's

band index $Y(t)$, which measures the segregation of opposite flow directions.[37] The band index $Y(t)$ is computed as follows. We first define a band B as a rectangular area extending longitudinally from one end of the street to the other and laterally from $y_1 = y_0$ to $y_2 = y_0 + d$, where d is the width of the rectangular area. Here, we use $d = 0.5$ m. The index $Y_B(t)$ for the band B is defined as $Y_B(t) = |n_1 - n_2|/(n_1 + n_2)$, where n_1 is the number of pedestrians belonging to one pedestrian stream within band B, and n_2 is the number of pedestrians belonging to the opposite flow. The band index $Y(t)$ is then defined as the average value of $Y_B(t)$, where y_0 is varied from 0 to $W - d$, W being the width of the street. In Fig. 22, y_0 is varied in steps of size $\Delta y = 0.1$ m. According to this definition, $Y(t) = 0$ for mixed counterflows and 1 for a perfect segregation of the opposite flows.

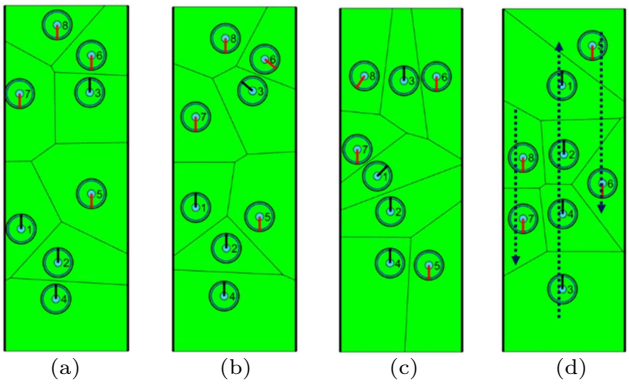


Fig. 21. The simulation snapshots of bidirectional pedestrian flow in the corridor. Eight pedestrians with opposite walking direction are randomly distributed in the 7 m × 2.5 m corridor. The vertical lines in the pedestrian circle represent the walking direction of pedestrians. In the beginning, the black ones indicate the walking direction from bottom to top of the corridor, and the red ones indicate the walking direction from top to bottom of the corridor.

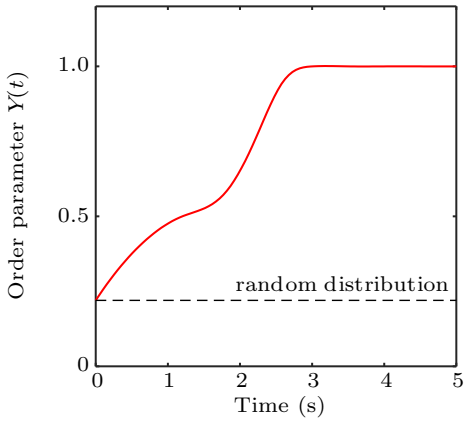


Fig. 22. Emergence of spatial segregation in a simulated of bidirectional pedestrian flow in the corridor. At time $T = 0$, eight pedestrians are randomly distributed in the corridor (four pedestrians in each flow direction). Under periodic boundary condition, after 3 s of the simulation the flows are fully segregated.

3.3. Walking through static obstacles

In a 10 m × 2.5 m corridor, we carry out the simulation of unidirectional pedestrian flow with static obstacles. Here, we set nine stationary pedestrians as static obstacles which randomly distributed in the corridor initially. And the location coordinates of the stationary pedestrians are (0.35, 1.71), (1, 1.71), (1.03, 3.83), (2.23, 3.17), (0.94, 5.24), (1.5, 5.25), (2.22, 6.95), (0.8, 8.05), (1.4, 8.06), respectively. Especially, we set a red detouring-pedestrian of (1.02, 0.39) in the center of the bottom of the corridor, and the target walking direction towards to the top of the corridor. Then during the moving progress, we can see the detouring-pedestrian would continuously detour others actively if the static obstacles are hindering the way of the detouring-pedestrian and the walking trajectory looks smooth, as shown in Fig. 23.

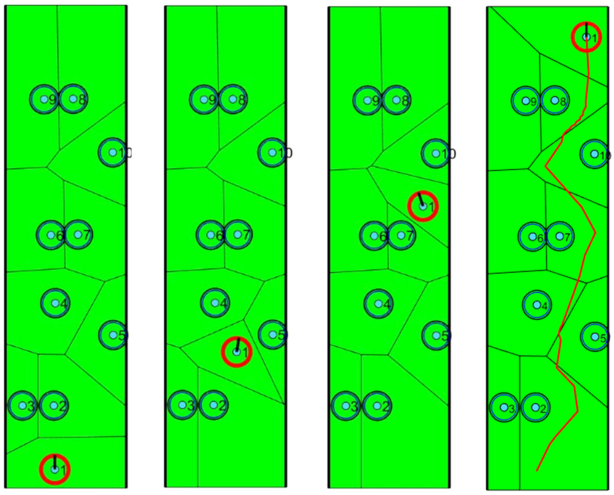


Fig. 23. The simulation snapshots of unidirectional pedestrian flow with a lot of static obstacles in the corridor. The black circles represent stationary obstacles, the red circle represents a walking pedestrian, and the red line represents the walking trajectory of the detouring-pedestrian.

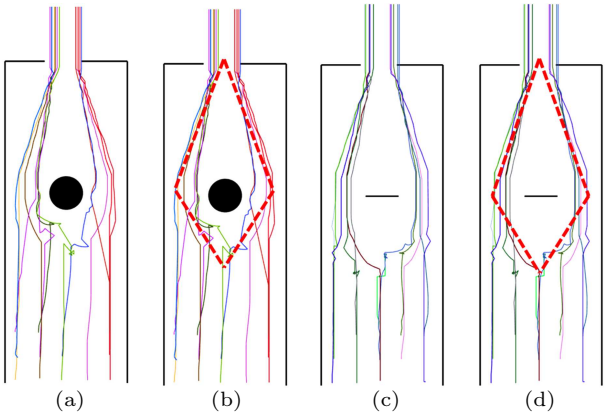


Fig. 24. The simulation snapshots of unidirectional pedestrian flow with a major obstacle in the corridor. (a) With a circle-shaped obstacle in the simulation process; (b) the avoiding area before the circle-shaped obstacle and the unoccupied area after the obstacle look like a rhombus; (c) with a bar-shaped obstacle in the simulation process; (d) the avoiding area before the bar-shaped obstacle and the unoccupied area after the obstacle look like a rhombus.

We also carry out a simulation of unidirectional pedestrian flow with a major obstacle of circle-shaped or bar-shaped in a 10 m × 3.5 m corridor. The difference with the last simulation is that we set twelve detouring-pedestrians that randomly distributed in the area of 2.5 m × 3.5 m at the bottom

of the corridor and one major big obstacle in the middle of the corridor. Then we can see that the walking trajectories of the detouring-pedestrians in Fig. 24. When the detouring-pedestrians detour the major obstacle, the avoiding area before the obstacle and the unoccupied area after the obstacle look like a rhombus can be observed in the pedestrian evading and surpassing process, as shown in Figs. 24(b) and 24(d).

3.4. A room with single-exit

By observing realistic scenarios and pedestrian experiments, we can find the difference of the crowd shape in front of a bottleneck from simulation results. The shape is semicircle arched in simulation, but in actual life scenarios, such as scenic spots, shopping malls and transportation hubs, we can observe that the fan-shaped when pedestrians crowd and evacuate in front of a bottleneck. For example, crowded pedestrians form the fan shape at each door of the subway train when pedestrians spontaneously queue or get on in sequence.

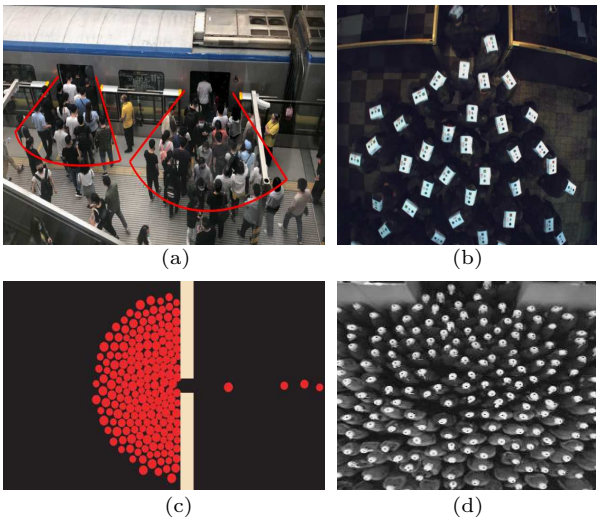


Fig. 25. Different shapes of pedestrians form before the bottleneck. (a) The fan-shaped can be seen in reality; (b) the fan-shaped can be seen in experiment;[54] (c) the semicircular arch can be seen in the simulation of the traditional SFM;[20] (d) the semicircular arch can be seen in experiment with the design.[55]

We took a photo at Xi'erqi station of Beijing subway during the morning rush hour as shown in Fig. 25(a). Furthermore, researchers did some experiments with pedestrians passing the bottleneck,[53,54] and found while pedestrians wait in sequence to pass through a narrow bottleneck, the crowd shape appeared like a fan, as shown in Fig. 25(b).[54] However, in the traditional SFM,[20] crowded pedestrians in front of the bottleneck present a semicircular arch, as shown in Fig. 25(c).[20] By contrast, some researchers did pedestrian experiments, and we can see pedestrians form a semicircular arch before the bottleneck,[55] however, of which at the beginning, crowded pedestrians already were designed to be crowded into an arch before the bottleneck, instead of spontaneous formation, as shown in Fig. 25(d).[55]

In order to observe the crowd gathering phenomenon in front of the bottleneck, we carry out the simulation of unidirectional pedestrian flow in a 14 m × 10 m room with the single exit. Especially, we set pedestrians could not get out of the single exit in the middle of the top of the room during the evacuation. Then we could see that pedestrians try to queue in an orderly manner at the exit. Besides, to make the walking target direction of pedestrians more realistic, we set the pedestrians who on the left side of the room would walk to the left side of the exit, who on the right side of the room would walk to the right side of the exit, and who facing the exit would walk straight ahead directly to the exit, as shown in the following Fig. 26.

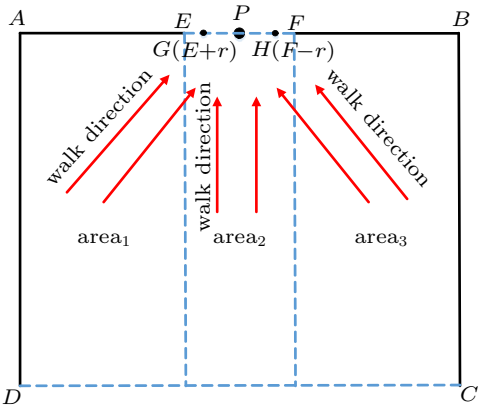


Fig. 26. The walking target direction of unidirectional pedestrian flow in a room with single-exit. Here r is the radius of pedestrians. And the pedestrians who in area$_1$ would randomly walk to the locations G–P, who in area$_2$ would walk straight ahead directly to the exit, and who in area$_3$ would randomly walk to the locations P–H.

In the beginning, the pedestrians are initially randomly generated within a range of 3 m × 10 m at the bottom of the room, as shown in Fig. 27(a). Since the space of the room is large enough, the pedestrians gradually diffuse and relatively far apart with each other during the walking process. At this time, the local density of each pedestrian is small and the pedestrians almost all have higher free-flow velocity magnitude, as shown in Fig. 27(b). Finally, when the simulation is stable, the pedestrians gathering before the sing-exit due to the narrow bottleneck would lead to the accumulation and blockage. Then we observe the pedestrians forming 4-5 layers orderly queues with almost standstill, and the crowd shape looks like fan-shaped which different from other traditional researches in the simulation. And our simulation result is similar to the actual situation, as shown in Fig. 27(c). However, the same simulation situation still forms the semicircular arch in the traditional SFM.

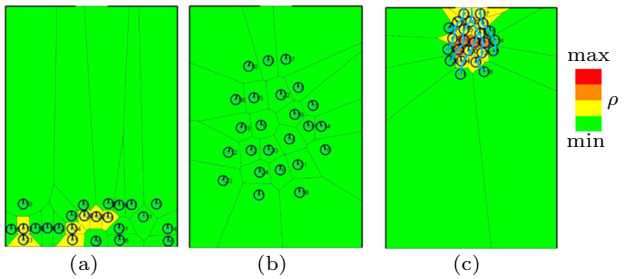


Fig. 27. The simulation snapshots of unidirectional pedestrian flow in a room with single exit.

There are 24 pedestrians randomly distributed at the bottom of the room initially. Then we could see the overall walking trajectories until the pedestrians keep standstill before the exit in Fig. 28. Furthermore, we make some surface plots of the unidirectional pedestrian flow, and we can see the relationship between the velocity–density and the locations of pedestrians, which corresponding to the walking trajectories at the different walking stages in Fig. 29. In the beginning, pedestrians almost all have high density and low velocity at the bottom of the room at $t = 0$ s. Whereas, due to have much more extensive personal space, some pedestrians near the periphery of the crowd have relatively lower density and higher velocity than others. Next, due to the diffusion of pedestrians, we can see several different layers of the density-velocity at $t = 7.6$ s. Finally, the pedestrians forming several orderly queues before the exit at $t = 20$ s. We can see the pedestrians have higher density, and lower velocity almost equals zero than before, and then the personal space of pedestrians near the periphery of the crowd is more comfortable and flexible at this time.

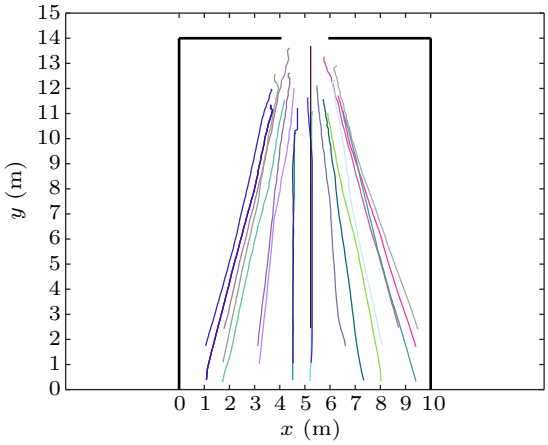


Fig. 28. The simulation snapshot of walking trajectories of unidirectional pedestrian flow in a room with single exit.

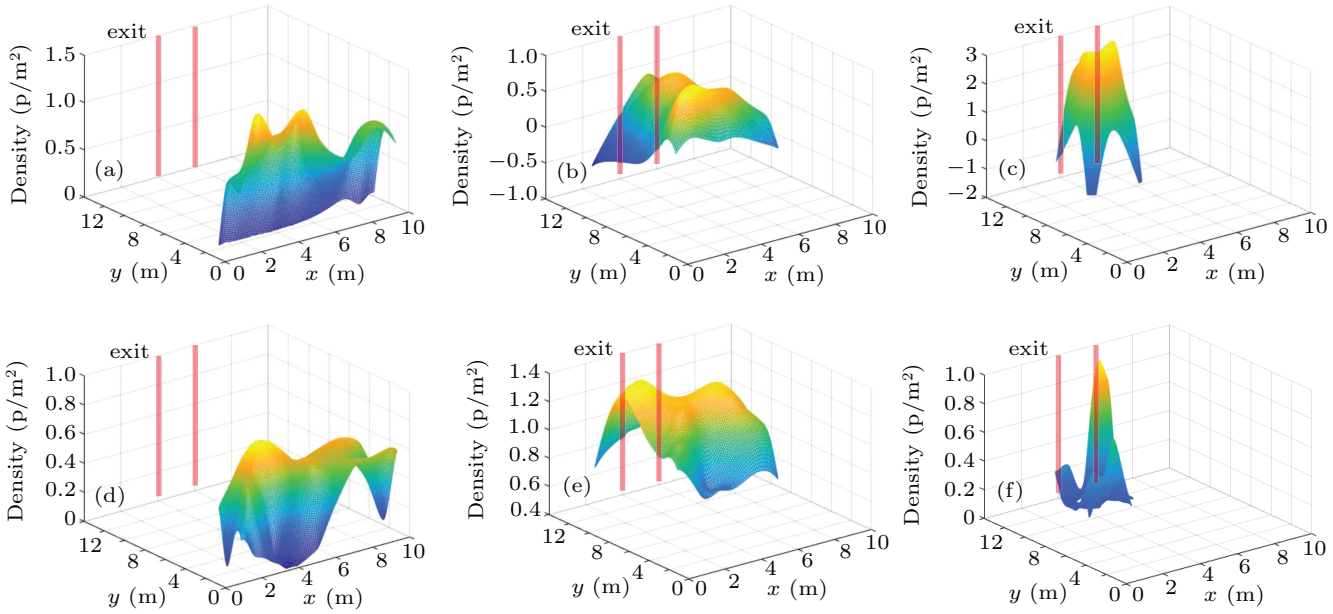


Fig. 29. The surface plots of unidirectional pedestrian flow. The relationship between the density and the locations of pedestrians at the different walking stages in panels (a), (b), (c), and the relationship between the velocity and the locations of pedestrians at the different walking stages in panels (d), (e), (f). And the red lines represent the location of the exit.

Generally, pedestrians usually make different choices to walk even in the same scene. Then due to the choice of pedestrian movement strategy has many factors in real scenarios, and the determination of pedestrian detour/follow behavior has the characteristics of uncertainty, complexity, and randomness, we carry out many simulations to study. To study the behaviors of pedestrians in the evacuation flow, we also simulate the unidirectional pedestrian flow in the room with single-exit, and pedestrians can get out of the exit when arriving in the door this time. To research the effect of the detour preference to the choice of pedestrian movement in the simulation, we set three kinds of ratio that the detour preference to the non-detour preference is 1:0, 1:1, or 0:1, respectively. And we would see the difference of the evacuation time with different number of pedestrians or different widths of the bottleneck in the same condition. Then, to obtain stable results, each simulation would be repeated 10 times. And the number of pedestrians is gradually increased from 12 to 48 with 6

pedestrians added each time, and the width of the bottleneck is gradually increased from 1.2 m to 2.4 m with 0.2 m added each time. Though the initial pedestrians are randomly generated in the room, the locations of the pedestrians are fixed at the beginning next. Then we could see the change of the evacuation time with the number of pedestrians in Fig. 30(a), and the change of the evacuation time with the widths of the bottleneck in Fig. 30(b).

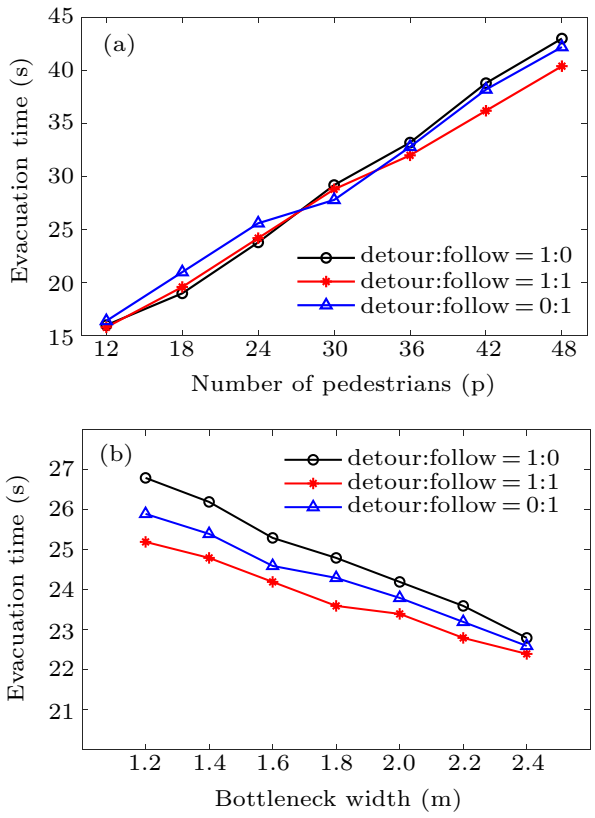


Fig. 30. The change of the evacuation time with the number of pedestrians or the widths of the bottleneck. The width of the bottleneck is 1.4 m in panel (a), and the number of pedestrians is 28 in panel (b).

We can observe that when the number of pedestrians is relatively small and most pedestrians who prefer to detour, the whole pedestrians would have less overall evacuation time. And when the number of pedestrians is relatively large and most pedestrians who prefer to follow, the whole pedestrians would have less overall evacuation time, as shown in Fig. 30(a). Besides, when some proper proportion of pedestrians choose to detour and the others not, the whole pedestrians would have higher overall evacuation efficiency and lower overall evacuation time. Moreover, we can observe that the overall evacuation time of pedestrians decrease with the increase of the bottleneck width no matter which movement behavior pedestrians choose, as shown in Fig. 30(b). Especially, if most pedestrians prefer to follow an orderly manner instead of to follow personal intend to detour, the whole pedestrians would have higher overall evacuation efficiency with the narrower bottleneck.

4. Conclusion

We propose a new heuristic model based on the Voronoi diagram to describe the choice of pedestrian walking behaviors. Based on the heuristic rules, we propose to consider the preference and willingness demand as detour intention scale to affect the willingness determination of detour or follow others, the safe demand as a microscopic anti-deadlock mechanism, and the fast and comfort demand as a site-fine-tuning mechanism. We propose calculation principles and a pair of "allow-areas and denial-areas" rule for confirmation of pedestrian detour directions. In the model, the pedestrian space is divided into a series of Voronoi cells. This model can avoid complex situation analysis and parameter calibration, consider all neighbors at the same time to avoid a group, solve the decision-making mechanism of the detour or follow behaviors, and then avoid collision and overlap phenomenon between pedestrians effectively. Moreover, this model can realize the behavior of active detour others and the balance of collision avoidance and minimizing the detour distances.

We verify the model by simulating many scenarios, such as unidirectional pedestrian flow, bidirectional pedestrian flow, with static obstacles in the corridor, and evacuation from a room with single-exit. The simulation results show that the model can achieve an excellent velocity–density relationship of pedestrians, reproduce reasonable self-organizing phenomena such as "lane formation," "fan-shaped before a bottleneck" and show realistic pedestrian detour behavior. When detouring others, the detouring-pedestrians detour both sides of neighbors or obstacles and then converge together which lead the avoiding area before the obstacle and the unoccupied area after obstacle look like a rhombus. In the simulation of evacuating and queuing in front of the bottleneck, we observe that the crowd shape is fan-shaped instead of arching which different from the simulation of the traditional SFM. We can see that the simulation results of our model are more real and reliable which can show the phenomenon of the crowd in order before the bottleneck realistically. By studying the pedestrian simulation with different walking intentions, we can see that when pedestrians move in a limited space, the behavior of orderly follow is more conducive to the improvement of the overall evacuation efficiency.

Although the model in this paper is performed well in the simulation due to the behaviors of pedestrians are very complicated and the perceptions and decisions of pedestrians are different in many scenarios we will consider to carry on the research on the characteristics of heterogeneous pedestrians, companion pedestrians, guidance information, a large-scale anti-deadlock mechanism, variety of obstacle layouts and variety of exit layouts. Besides, we also need to research how to improve our model to enhance the simulation efficiency to

adapt large-scale pedestrian flow in complex situations in the future.

References

[1] Yang L, Rao P, Zhu K, Liu S and Zhan X 2012 *Saf. Sci.* **50** 1173
[2] Shiwakoti N and Sarvi M 2013 *Transp. Res. Part C* **37** 260
[3] Guo R Y, Huang H J and Wong S C 2011 *Transp. Res. Part B* **45** 490
[4] Johansson A, Batty M, Hayashi K, Al B O, Marcozzi D and Memish Z A 2012 *Lancet Infect. Dis.* **12** 150
[5] Shiwakoti N, Tay R, Stasinopoulos P and Woolley P J 2017 *Saf. Sci.* **91** 40
[6] Duives D C, Daamen W and Hoogendoorn S P 2013 *Transp. Res. Part C* **37** 193
[7] Zheng X, Zhong T and Liu M 2009 *Build. Environ.* **44** 437
[8] Xiao Y, Gao Z Y, Qu Y C and Li X G 2016 *Transp. Res. Part C* **68** 566
[9] Blue V and Adler J 2000 *Transp. Res. Record* **1710** 20
[10] Yanagisawa D, Nishi R, Tomoeda A, Ohtsuka K, Kimura A, Suma Y and Nishinari K 2011 *Sice Jcmsi.* **3** 395
[11] Zhu K, Yang Y and Shi Q 2016 *Simul. Model. Pract. Theory* **69** 31
[12] Yue F R, Chen J, Ma J, Song W G and Lu X M 2018 *Chin. Phys. B.* **27** 124501
[13] Lu L L, Ren G, Wang W and Wang Y 2014 *Chin. Phys. B* **23** 088901
[14] Burstedde C, Klauck K, Schadschneider A and Zittartz J 2001 *Physica A* **295** 507
[15] Liu S, Yang L, Fang T and Li J 2009 *Physica A* **388** 1921
[16] Li M H, Yuan Z Z, Xu Y and Tian J F 2015 *Acta Phys. Sin.* **64** 018903 (in Chinese)
[17] Yue H, Zhang B Y, Shao C F and Xing Y 2014 *Chin. Phys. B* **23** 050512
[18] Yue H, Wang S, Jia X L, Li J and Shao C F 2016 *Simul.-Trans. Soc. Model. Simul. Int.* **92** 491
[19] Zhang L, Yue H, Li M, Wang S and Mi X Y 2015 *Acta Phys. Sin.* **64** 060505 (in Chinese)
[20] Helbing D, Farkas I and Vicsek T 2000 *Nature* **407** 487
[21] Helbing D, Buzna L, Johansson A and Werner T 2005 *Transp. Sci.* **39** 1
[22] Lakoba T I, Kaup D J and Finkelstein N M 2005 *Simul. Trans. Soc. Model. Simul. Int.* **81** 339
[23] Yang X X, Dong H R, Wang Q L, Chen Y and Hu X M 2014 *Physica A* **411** 63
[24] Hou L, Liu J G, Pan X and Wang B H 2014 *Physica A* **400** 93
[25] Seer S, Rudloff C, Matyus T and Brändle N 2014 *Conference on Pedestrian and Evacuation Dynamics (PED)*, October 22–24, 2014, Delft, Netherlands
[26] Seer S, Brändle N and Ratti C 2014 *Transp. Res. Part C* **48** 212
[27] Kretz T 2015 *Physica A* **438** 272
[28] Yang X X, Dong H R, Yao X M and Sun X B 2016 *Chin. Phys. B* **25** 128901
[29] Wang L, Zheng J H, Zhang X S, Zhang J L, Wang Q Z and Zhang Q 2016 *Chin. Phys. B* **25** 118901
[30] Parisi D R, Gilman M and Moldovan H 2009 *Physica A* **388** 3600
[31] Frank G A and Dorso C O 2011 *Physica A* **390** 2135
[32] Zhao Y X, Li M F, Lu X, Tian L J, Yu Z Y, Huang K, Wang Y N and Li T 2017 *Physica A* **465** 175
[33] Rudloff C, Matyus T, Seer S and Bauer D 2011 *Transp. Res. Record* **2264** 101
[34] Moussaïd M, Helbing D, Garnier S, Johansson A, Combe M and Theraulaz G 2009 *Proc. R. Soc. B, Biol. Sci.* **276** 2755
[35] Lv W, Song W G, Ma J and Fang Z M 2013 *IEEE Trans. Intell. Transp. Syst.* **14** 1753
[36] Jia X L, Yue H, Tian X and Yin H H 2017 *Simul. Trans. Soc. Model. Simul. Int.* **93** 1013
[37] Moussaïd M, Helbing D and Theraulaz G 2011 *Proc. Natl. Acad. Sci. USA* **108** 6884
[38] Degond P, Appert-Rolland C, Moussaïd M, Pettre J and Theraulaz G 2013 *J. Stat. Phys.* **152** 1033
[39] Guo R Y 2014 *Physica A* **415** 428
[40] Guo W, Wang X L and Zheng X P 2015 *Physica A* **432** 87
[41] Guy S J, Curtis S, Lin M C and Manocha D 2012 *Phys. Rev. E* **85** 016110
[42] Qu Y C, Xiao Y, Wu J J, Tang T and Gao Z Y 2018 *Physica A* **492** 1153
[43] Seyfried A, Steffen B and Lippert T 2006 *Physica A* **368** 232
[44] Li S S, Qian D L and Wang J Z 2012 *J. Jilin Univ., Eng. Technol. Ed.* **42** 623
[45] Qu Y C, Gao Z Y, Orenstein P, Long J C and Li X G 2015 *Transportmetrica B-Transp. Dyn.* **3** 1
[46] Marjorie D 1993 *Science* **260** 1170
[47] Fruin J J 1971 *Pedestrian and Planning Design* (New York: Metropolitan Association of Urban Designer and Environmental Planners Inc.)
[48] Older S J 1968 *Traff. Eng. Contr.* **10** 160
[49] Mōri M and Tsukaguchi H 1987 *Transp. Res. Part A* **21** 223
[50] Zhang J, Klingsch W, Schadschneider A and Seyfried A 2011 *J. Stat. Mech. -Theory Exp.* **6** P06004
[51] Weidmann U 1993 *Transporttechnik der Fussgänger: Transporttechnische Eigenschaften des Fussgängerverkehrs* (Literaturauswertung) (Zurich: ETH, IVT)
[52] Hankin B D and Wright R A 1958 *Oper. Res. Q.* **9** 81
[53] Hoogendoorn S P and Daamen W 2005 *Transp. Sci.* **39** 147
[54] Liddle J, Seyfried A, Klingsch W, Rupprecht T, Schadschneider A and Winkens A 2009 arXiv: 0911.4350 [Physics.soc-ph]
[55] Liao W C, Seyfried A, Zhang J, Boltes M, Zheng X P and Zhao Y 2014 *Conference on Pedestrian and Evacuation Dynamics (PED)*, October 22–24, 2014, Delft, Netherlands